

STRUCTURE AND RHEOLOGICAL PROPERTIES OF POLY(VINYL CHLORIDE) MELTS

J. Lyngaae-Jørgensen

Instituttet for Kemiindustri, Bygning 227, the Technical
University of Denmark, 2800 Lyngby, Denmark.

Abstract - In order to interpret anomalous rheological data for poly(vinyl chloride) (PVC) samples relations between molecular structure and rheological functions for melts where the single polymer molecules constitute the flow units (monomolecular melts) are presented. It is shown that the viscosity function for PVC materials in simple shear flow coincide with a master curve for high density polyethylene (HDPE) samples. This master curve is given as a relation between a reduced viscosity and a reduced shear rate. It is inferred that monomolecular melt flow data for PVC materials may be predicted from master curve data for HDPE samples. Finally it is shown that the particle structure in emulsion polymers does disappear under continuous shear at 190°C if sufficient processing time is allowed. However, the time for interface destruction for emulsion polymers is much longer than for bulk polymers.

INTRODUCTION, STRUCTURE OF PVC MATERIALS

The rheological data reported in the literature have been extensively reviewed by Pezzin (1) in 1970 and Collins in 1976 (2). The structure factors influencing the properties of a polymer material can be systematically described by describing the molecular structure, the microstructure and the macrostructure of a polymer material. "Molecular structure" refers to the way the single polymer molecules are built, the microstructure refers to deviations from a fictitious reference state which is a stress free, isotropic, amorphous homogeneous equilibrium state of pure homopolymer with a given molecular structure. The macrostructure of a material is defined by the outer geometrical form of a given sample. This distinction is primarily useful when dealing with thermoplastic materials because each polymer molecule can be considered as an entity which (at least in principle) retains its identity during processing. Experimental data for PVC compounds in simple stationary flow fields are not in agreement with the behaviour for polymer melts where the single polymer molecules constitute the flow units. Such melts will be referred to as monomolecular melts in the following text. The molecular structure of PVC materials is, however, rather simple.

The structure of polymer materials produced at temperatures above 20°C are normally determined by transfer to monomer which results in a molecular weight distribution almost identical with the most probable distribution (3, 4). Unless special production methods are used (5), a product having almost no long chain branching is obtained (6-9).

The products contain short branches exclusively or predominantly of the methylchloride type ($-\text{CH}_2\text{Cl}$) (10, 11). The tacticity of the material seems to be determined almost exclusively by the polymerization temperature (12, 13), and the degree of syndiotacticity, which is approximately 0.53 for samples prepared at 50°C, increases with decreasing polymerization temperature.

The deviations from monomolecular melt flow behaviour found in the literature are caused by several factors. The most important factors causing anomalous rheological measurements seem to be related to the microstructure and the macrostructure of the PVC melt.

The macrostructure of the PVC particles produced depends on the polymerization conditions (8). A rough classification could be:

- Materials produced by emulsion polymerization consist normally of more or less coherent clusters of emulsion particles.

- Materials produced by bulk polymerization consist of "aggregates" of the so-called primary particles with dimensions of about 1μ .

- Materials produced by suspension polymerization consist of suspension particles which are covered by a more or less fractured skin of suspension aid (e.g. a skin of polyvinylalcohol probably with grafted PVC chains) and contain a more or less porous structure consisting essentially of primary particles. The most important microstructural factor of PVC materials seems to be the crystallinity. As early as 1949 Alfrey et al. (14) realized that the behaviour of PVC samples in stress-relaxation seemed to indicate the existence of a crystalline network in PVC samples. However, systematic investigations began much later. Evidence for crystallinity in PVC came from many sources such as X-ray investigations, DTA measurements and IR measurements (13, 15). Pezzin (1) pointed out very strongly that the crystallinity of PVC samples was a key parameter in determining the rheological properties.

The fact that PVC materials form stable crystallite aggregates in dilute solutions with a branched structure of single molecules held together by a crystalline nucleus (16) and that the melting points of these crystallites can be predicted using classical thermodynamical methods (17), lends further support regarding the importance of crystallinity in PVC.

There exist some discrepancies in the literature concerning both the dimensions of the unit cell and the stereoregularity requirements for crystallinity (13, 15). Until recently, it was assumed that only the syndiotactic part could be incorporated in crystalline parts of the materials, but recently Juijn et al. have proposed a model where both isotactic and syndiotactic parts of the molecules may crystallize in the same crystal lattice (18).

However, it is commonly agreed that most commercial PVC materials (i.e. materials produced between say 40-70°C) have low crystallinity (in the area between 5-20% by volume).

The melting range is very broad indeed, stretching from approximately 130°C to approximately 230°C for materials produced between 40 and 70°C.

Since PVC is thermally unstable it has to be processed below its melting point (1).

Furthermore, in the compounding process a large number of ingredients such as fillers, stabilizers, plasticizers, lubricants, etc. are added to PVC materials in order to optimize the properties of the product.

Thus, in processing of PVC materials one is faced with a material with a very complex structure, which may be described as:

Molecular structure: The PVC materials may be treated as materials without long branches and with the most probable molecular weight distribution.

Microstructure: Most commercial samples have 5-20% crystallinity. It may be assumed that the fringed micelle model gives a reasonable representation of the crystallite structure in PVC materials. All compounds contain stabilizers (19) just under half of all commodities produced contain different amounts of plasticizers. Rigid compounds particularly contain lubricants and fillers. For special compounds, blow agents etc. may be added.

The macrostructure of the materials as produced consists of agglomerates of particles. These particles seem to be relatively stable below the melting temperature of the three-dimensional network which apparently stabilizes the particle structure (20-23).

Considering the complexity of the structure of PVC materials taken together with the fact that most compounds are insufficiently stabilized and that slip agents are deliberately added to give easier processing, it is hardly surprising that rheological data on PVC compounds are often inconsistent.

A common consensus concerning the flow units and flow mechanisms for PVC compounds processed below the static melting point has not yet been achieved.

However, most authors agree that the presence of a certain amount of crystallinity persisting in the melt state is at least a contributory cause for many of the various anomalies observed in the study of PVC melts.

Other factors such as for example the breakdown of the no slip condition at the wall of rheometers and process equipment (24), non-isothermal flow conditions, particle flow and melt fracture, further complicate the study of PVC melts.

For such complex systems this author believes that it is extremely useful to be able to predict the behaviour of a monomolecular melt under the same processing conditions and use this predicted behaviour for a reference purpose. The distinction between non-stationary and stationary flow cases seems to be even more critical for melts of complex materials than for the melts of homopolymers.

In the following text a distinction between measurements corresponding to achievement of stationarity or steady state equilibrium and non-steady state

measurements is maintained.

Steady state equilibrium data can (at least in principle) be obtained from those rheometers allowing infinite shearing. The distinction is necessary because the breakdown of the micro- and especially the macrostructure in PVC compounds can be a slow process compared with the final residence time in much processing and measuring equipment. If structure breakdown influences the measurements, interpretation of the results is greatly impeded.

STEADY STATE EQUILIBRIUM FLOW

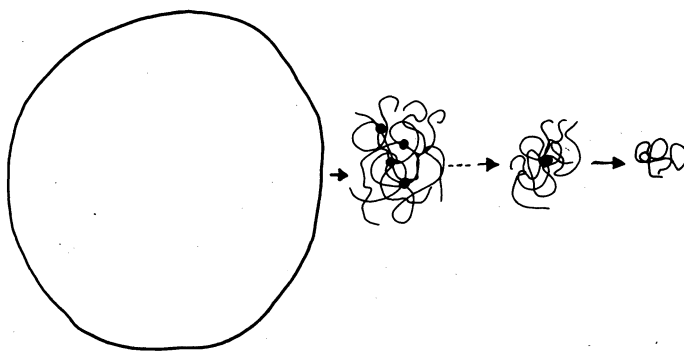
Only equipment which permits continuous shearing can secure the attainment of a stationary flow with a characteristic limiting melt structure. Only this last case will be considered under stationary flow in the following. In principle cone and plate geometry is best suited for the study of such time dependent behaviour. However, the severe limitations of this geometry makes the use of other geometries with rather ill-defined flows - such as the bicone geometry-necessary.

In the following we consider systems under stationary flow conditions, where degradation does not take place, where the no slip condition is fulfilled and where the original particle structure is destroyed.

Melting of Crystallite Aggregates in Simple Stationary Shearing Flow Fields Below the Static Melting Point

The melting temperature (T_m) of a crystalline material is defined as the temperature at which the last trace of crystallinity disappears.

A possible description of an isothermal start-up experiment performed at temperatures greatly in excess of the glass transition temperature but below the static melting temperature for a prepressed PVC powder in simple shearing flow might be as follows: Suppose that the no slip condition normally used in evaluation of rheological experiments is valid. Furthermore, suppose that we have a suspension polymer with a highly irregular particle structure. Now through interfacial diffusion the interfaces will be interpenetrated. A flow process involving highly irregular particles of different sizes as flow units is impossible to imagine (force and momentum balances on such a particle flow cannot balance) and the formation of a slip plane in the material seems to be impossible without melt fracture. Thus the original particle structure will be broken down to still smaller aggregates of PVC molecules held together by the remaining parts of the three-dimensional network of crystallites (25). Before the last crystallite disappears, aggregates of the type shown on the sketch consisting of several polymer molecules held together by a crystalline nucleus are postulated to exist in the melt. These aggregates have the same structure as the most stable aggregates found in dilute solution (16).



A criterion function for the destruction of the last trace of crystallinity under simple shear flow conditions have been derived by the author in ref. 26.

The expression has the form

$$1/T_{\text{dyn}} - 1/T_m = \frac{\tau^2}{Q \cdot T_{\text{dyn}}^2} \quad (1)$$

where T_{dyn} is the melting temperature under shear flow conditions, τ is the shear stress (τ_{21}) and Q is an adjustable constant. Even though this expression was based on rather dubious arguments an expression of the same limiting form without adjustable parameters can be derived (27).

The expression has the form:

$$1/T_{\text{dyn}} - 1/T_m = \frac{\tau^2 - \tau}{QT_{\text{dyn}}^2} \quad (2)$$

which for $\tau \gg 1$ is identical with eq. (1)

$$\text{where } Q = \frac{2 c^3 R \Delta H_u}{V_u \rho^2 M_c H^2 a^2}$$

c is the polymer concentration, R is the gas constant, V_u is the molar volume of a repetition unit, ρ is the density, M_c is twice the molecular weight between entanglements, H is the ratio between the molecular weight by weight and the molecular weight by number and a is a dimensionless constant found from the viscosity function of monomolecular melts. ($a \approx 10$).

Molecular structure and Rheological Properties of Monomolecular Melts of PVC Compounds

Recently a number of solutions concerning the rheological functions in stationary simple shear flow, stationary extensional flow, dynamic experiments, initial behaviour in simple extensional flow etc., have been worked out for monomolecular melts of linear polymers (27).

For high density polyethylene (HDPE) and polypropylene (PP) samples a "master curve" for the viscosity (η) function in stationary simple shear flow is shown as the solid line on fig. 1. The solution is given as a reduced viscosity (η/η_0) as a function of reduced shear rate ($\lambda\dot{\gamma}$), where η_0 is the zero shear viscosity, $\dot{\gamma}$ is the shear rate and

$$\lambda = \frac{\eta_0 M_c \cdot H \cdot \rho}{c^2 RT}$$

T is the absolute temperature and the rest of the symbols are defined above.

Fig. 1 shows a plot of experimental data for PVC compounds measured under conditions predicted to correspond to a monomolecular melt state according to eq. (1).

Plasticized samples should deviate from the master curve at higher shear rates (27). It may therefore be inferred that the rheological functions for monomolecular melts of PVC compounds can be predicted using master curves for HDPE (and/or PP) samples.

This is a useful result since data for high density polyethylene are quite abundant in the literature and since measurements on high density polyethylene in the monomolecular melt state are much easier to obtain than data for monomolecular PVC melts.

The dynamic viscosity functions for monomolecular melts of PVC may be predicted from fig. 1 since the reduced real (η') and imaginary (η'') viscosities give the same curve as shown on fig. 1 when η'/η_0 and/or η''/η_0 (for $\lambda\omega > 0.1$) are plotted against $2\lambda\omega$ for HDPE. ω is the angular frequency. Thus the prediction is obtained by substitution of the abscissa $\lambda\dot{\gamma}$ with $2\lambda\omega$.

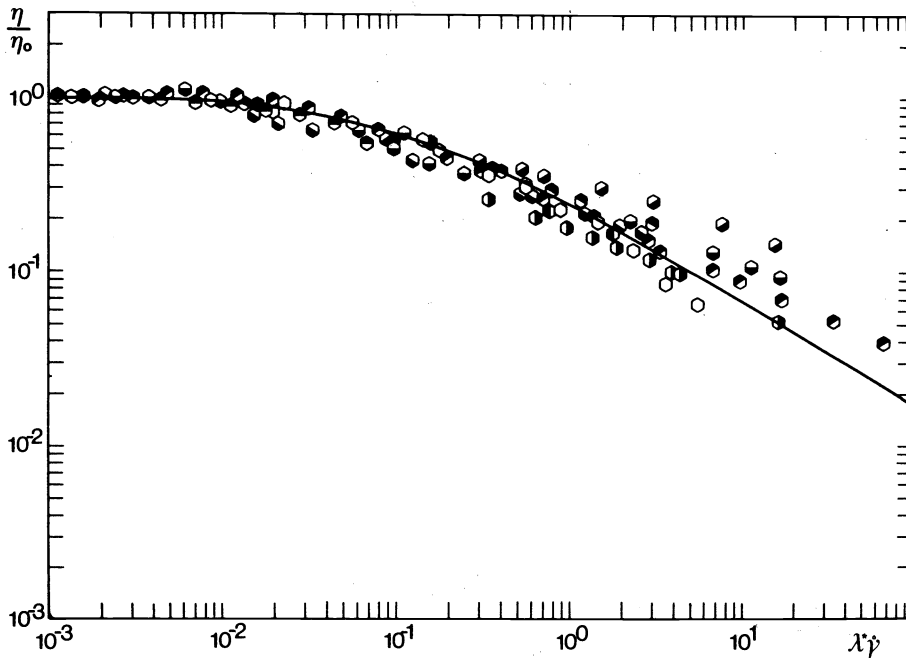


Fig. 1 show a plot of reduced viscosity against reduced shear rate for PVC compounds. Rigid PVC: \bullet $T=230^{\circ}\text{C}$ ref. 28, \blacklozenge $T=240^{\circ}\text{C}$ ref. 28, \blacklozenge $T=230^{\circ}\text{C}$ ref. 29, \circ $T=239^{\circ}\text{C}$ ref. 30.
 PVC/DOP: \blacklozenge $T=220^{\circ}\text{C}$, $c=0,5$, $\bar{M}_w=166000$, \blacklozenge $T=195^{\circ}\text{C}$, $c=0,5$, $\bar{M}_w=70000$, \blacklozenge $T=210^{\circ}\text{C}$, $c=0,708$, $\bar{M}_w=7000$, \blacklozenge $T=210^{\circ}\text{C}$, $c=0,708$, $\bar{M}_w=110000$, all ref. 29, \bullet $T=239^{\circ}\text{C}$, $c=0,933$, $\bar{M}_w=96000$, ref. 30.
 PVC/TTP: \blacklozenge $T=195^{\circ}\text{C}$, $c=0,554$, $\bar{M}_w=70000$ ref. 29

NON-STATIONARY FLOW OF PVC MATERIALS

Melt Fracture Phenomena in PVC Materials

Vinogradov (31-34) has shown that fracture in polymer melts can be described in much the same way as fracture in lightly crosslinked rubbers. T.L. Smith (35) has reviewed the topic of fracture mechanisms in elastomers and shown that

$$\log \tau_{cr} \left(\frac{T}{T_{ref}} \right) \text{ against } \log (\dot{\epsilon} a_T)$$

is a master curve for a given rubber where τ_{cr} are the breaking stress, a_T the WLF shift factor and $\dot{\epsilon}$ is the rate of deformation.

Furthermore Bueche (36) predicts that the tensile strength is proportional to the number of network chains per unit volume to the power 2/3 at equivalent conditions of rate and temperature.

Based on the work of Vinogradov Bueche and Smith, a hypothesis of the following form has been shown to be reasonable (27): a delineation of

$$\tau_{cr}^s \left\{ \left(\frac{\rho}{M_c} \right)_{PE} \left(\frac{M_c}{c} \right) \right\}^{2/3} \text{ against } a_T \dot{\gamma}_{cr}^s$$

represents "spurt" fracture data of linear polymer materials. According to Vinogradov spurt fracture means fracture at the wall in the capillary of a

capillary rheometer. a_T is the WLF shift factor and τ_{cr}^s and $\dot{\gamma}_{cr}^s$ are the spurt fracture stress and spurt fracture shear rate respectively.

$\left\{ \left(\frac{\rho}{M_c} \right)_{\text{reference}} \cdot \left(\frac{M_c}{Z} \right) \right\}$ is a reduced entanglement density.

Spurt data for PVC data are shown on fig. 2 with symbols of the form. The solid line represents an empirical estimate of the spurt fracture master curve.

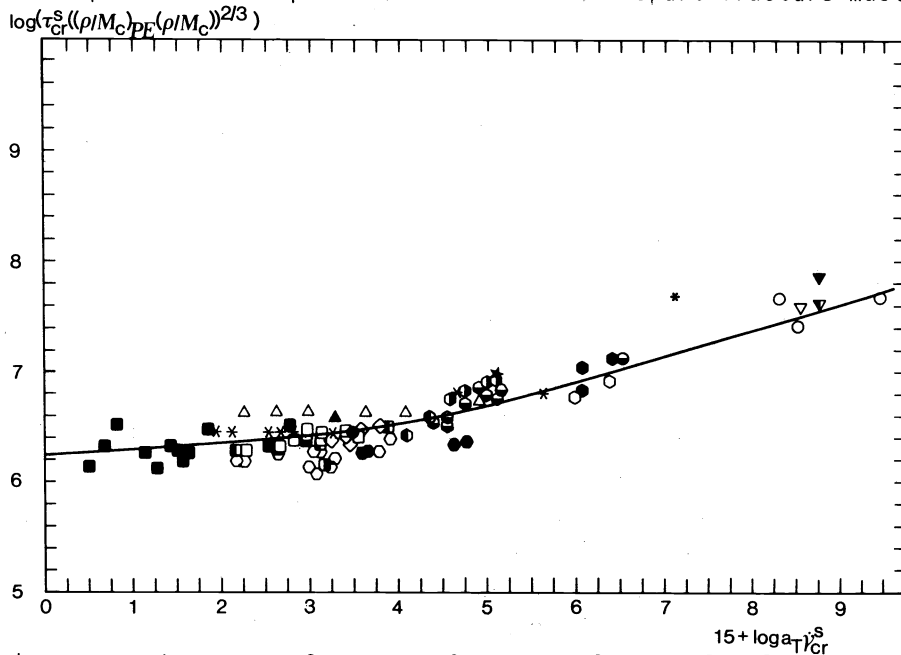


Fig. 2 shows a master curve for spurt fracture of monomolecular melts. \circ PVC data from ref. 38, \bullet PVC data from 25, \ominus PVC in DOP, data from ref. 39, \bullet PVC data from ref. 40, \ominus PVC in DOP, data from ref. 40. Other symbols various other polymers.

According to Vinogradov the spurt fracture should be observable in a flow curve as a point where the slope change abruptly to zero. Some literature data for spurt fracture have been estimated from the flow curve. Such a procedure may be misleading since thermal effects may lead to approximately the same behaviour. However, Bonnebat and deVries (37) obtain a limiting behaviour with zero slope in dynamic experiments where the heat dissipated is negligible under conditions which are predicted to give melt fracture (27). The data shown on fig. 2 roughly correspond to the spurt fracture behaviour predicted for monomolecular melts. This fact may be interpreted as a consequence of a complete melting of crystallite areas in PVC compounds at sufficiently high shear stresses as predicted by eq. 1.

A discontinuity in the energy of activation has been observed, first by Collins and Krier (28), and later confirmed by many investigations (eg. in a plot of viscosity against reciprocal temperature with shear rate as discrete variable). Fig. 3 is a double logarithmic plot of shear stress against $a_T \cdot \dot{\gamma}_{cr}$ showing corresponding values of shear stress, shear rate and temperature corresponding to the points where the energy of activation shows an abrupt change for samples which fracture in regions predicted to represent monomolecular melt state according to eq. (1).

The solid line represents the spurt fracture curve for monomolecular

melts of PVC.. $\left\{ \log \left(\tau_{cr}^s \left(\frac{\rho}{Z} \right)^{2/3} \right) \text{ against } 15 + \log a_T \dot{\gamma}_{cr} \right\}$.

Since the points scatter around the spurt fracture master curve we propose that the abrupt change of energy of activation is another reflection of melt fracture in the capillary.

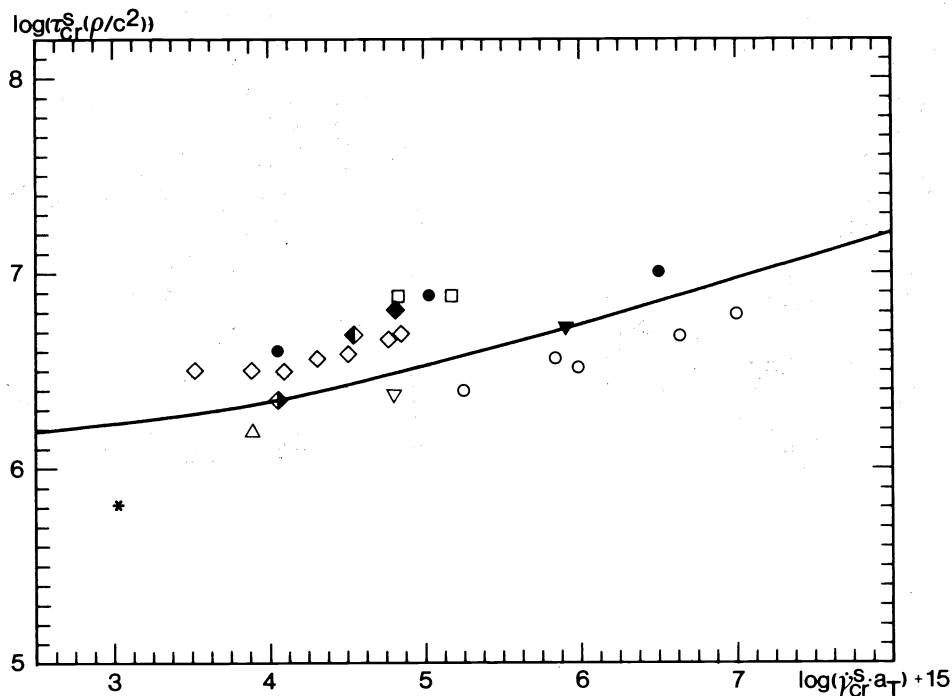


Fig. 3 shows a comparison between predicted spurt stress data for PVC materials (solid line) with data corresponding to the break points in plots of $\log \eta$ against $1/T$ for samples which show melt fracture in the monomolecular melt state (according to eq. 1). Collins and Metzger (41); ○ sample A; ● sample D. Sieglaff (42), ▽ 100 sec^{-1} , ▾ 1000 sec^{-1} . Collins and Krier (28), ◇ Geon 101EP, ◆ Diamond 450, ◆ Emulsion PVC, ◆ Geon 432 (5wt% VAc). Rasmussen (39), △ Corvic D65/8/DOP (100/40). Original data from Berens and Folt (22) retreated in ref. (41) □. Sieglaff (42) * 1 sec^{-1} , fracture is reported in the area corresponding to a melt state with stable crystallites.

The Influence of Structure on the Initial Response in Simple Shearing Flow

To study the effect of "structure" on the initial response and equilibrium flow in simple shearing isothermal flow, samples with different original macro- and microstructure were investigated. The investigations were performed at 190°C in bicone geometry using a Rheometrics mechanical spectrometer. Absolute values of shear stress could normally be reproduced within a standard deviation equal to 25% but occasionally deviations as large as three times the average of other measurements performed under the same conditions were observed. Since this effect is unexplained such data are not reliable. Measurements were performed on sintered samples of a bulk polymer, a suspension polymer, two emulsion polymers, a lightly crosslinked emulsion polymer and on samples where the particle structure was destroyed. The main result of this investigation is: All the samples give overshoot in the investigated shear rate interval between 0.01 sec^{-1} and 1 sec^{-1} . The shear value ($\dot{\gamma} \cdot t$) measured on materials which are originally at rest corresponding to the overshoot maximum (γ_{max}) is the same (within experimental uncertainty) for the investigated samples. γ_{max} is approximately 2.2 ± 0.2 . This value is slightly lower than the average value found for monomolecular melts which is $\gamma_{\text{max}} = 2.9$. Overshoot is observed in monomolecular melts for $\lambda \dot{\gamma} > 0.2$ (27).

Particle destruction during continuous shear flow at 190°C. The breakdown of structure during the experiments was followed by interrupting the experiments at different times and investigating the samples by electron microscopy. Two different techniques were used. One was scanning electron microscopy on fracture surfaces prepared at liquid nitrogen temperature. Alternatively, ultramicrotomic cuts through samples embedded in polymethylmethacrylate were made, a technique described by Hatori et al. (23). The breakdown of a bulk polymer (A) Vinnol Y60 and an emulsion polymer (C) with average diameter 0.27 μ was compared.

Fig. 4 and 5 show scanning pictures of a sintered sample of polymer A, fig. 6 shows a transmission picture of this sample. The particle structures are clearly revealed.

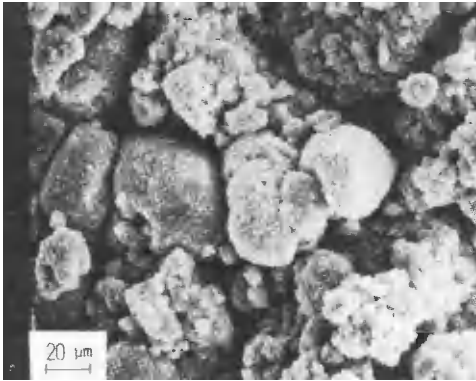


Fig. 4 .

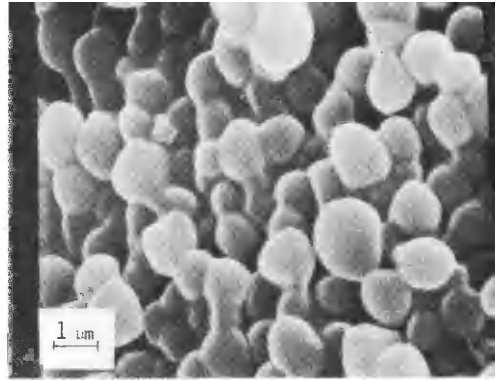


Fig. 5

Fig. 4 and 5 show scanning pictures of a sintered sample of a bulk polymer (sample A).

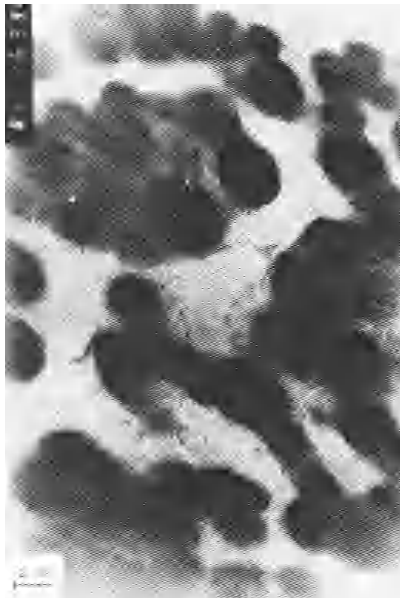


Fig. 6 shows a transmission picture of a sintered sample of a bulk polymer (sample A).

Fig. 7 show a transmission picture of polymer A.

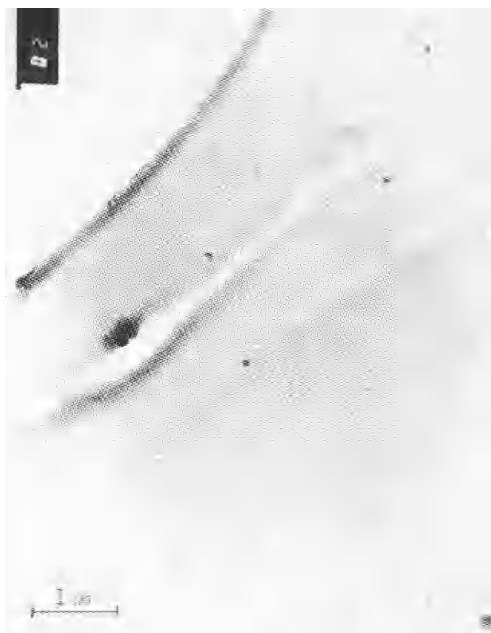


Fig. 7 shows a transmission picture of sample A after dissolution in THF and evaporation of the solvent.

This sample had been dissolved in tetrahydrofurane (THF) and the THF subsequently removed by evaporation. The ultramicrotomic cut was then prepared after PMMA embedding.

Fig. 8 shows a scanning picture of polymer A after sintering and processing in the bicore for 2.5 min at 190°C and $\dot{\gamma} = 0.063 \text{ sec}^{-1}$.

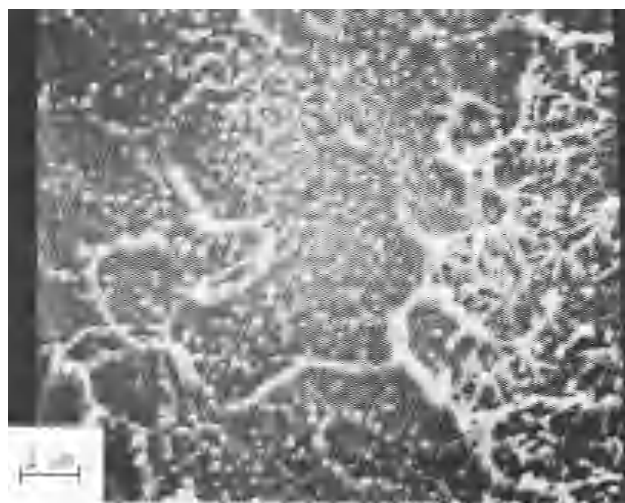


Fig. 8 shows a scanning picture of polymer A after processing in the bicore for 2.5 min. at 190°C and $\dot{\gamma} = 0.063 \text{ sec}^{-1}$.

Pictures resembling fig. 8 could be reproduced even for samples processed for 20 minutes or more. The corresponding transmission pictures as well as transmission pictures on pure PMMA were empty (without contrasts). It is clearly apparent that what appear to be perfectly spherical particles in

the fracture surface are in fact the circumferences of strings pulled out of the surface during fracture which when looked upon perpendicular to the strings appear as a cut-down forest of tree-stumps. This interpretation is supported by the fact that the same type of surface pattern can be observed in fracture surfaces of polystyrene as reported by Hayward (43, 44).

This investigation has shown that the original particle structure in bulk PVC are completely destroyed in a shear flow field. The investigations indicate that the particles loose their identity before the torque maximum is reached. Fig. 9 and 10 shows scanning and transmission pictures of (emulsion) polymer C.

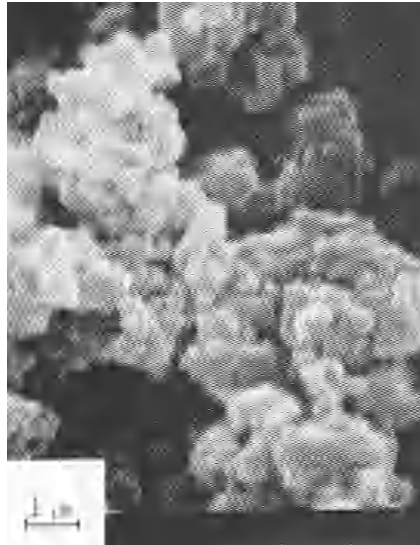


Fig. 9 shows a scanning picture of a sintered emulsion polymer with mean particle diameter: 0.27μ (sample C).

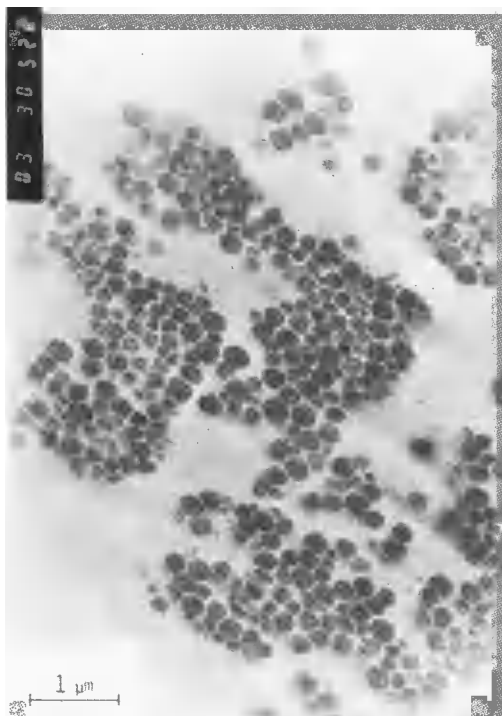


Fig. 10 shows a transmission picture of a sintered emulsion polymer (sample C).

After processing 3 min at 190°C and $\dot{\gamma} = 0.04 \text{ sec}^{-1}$ particles can still be distinguished in approximately half the scanning, as well as the transmission pictures as seen in fig. 11 and 12. The rest of the pictures were empty.

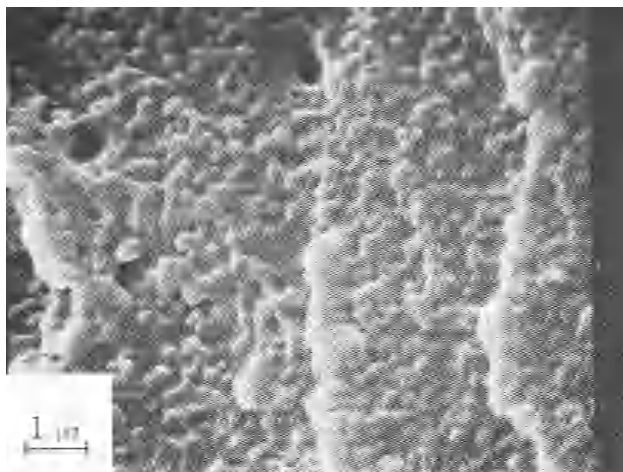


Fig. 11 shows a scanning picture of sample C after processing for 3 min. in the bicone at 190°C and $\dot{\gamma} = 0.04 \text{ sec}^{-1}$.



Fig. 12 shows a transmission picture of sample C after processing for 3 min. in the bicone at 190°C and $\dot{\gamma} = 0.04 \text{ sec}^{-1}$.

The occurrence of particles seems to spread over continuous areas in the sample.

Even in samples processed at $\dot{\gamma} = 0.04 \text{ sec}^{-1}$ at 190°C for 18 min a few scanning pictures could be found which seems to reveal the original particle structure as seen on fig. 13. However, transmission pictures were empty.

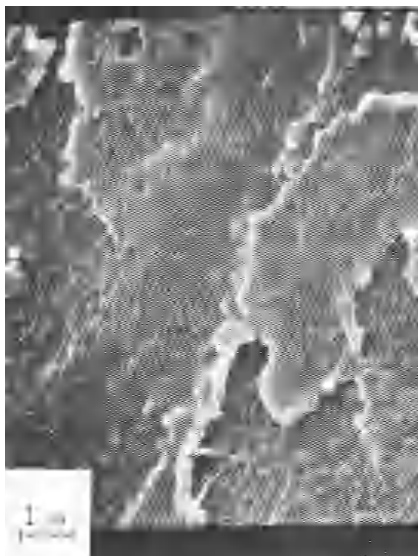


Fig. 13 shows a scanning picture of sample C after processing for 18 min. in the bicone at 190°C and $\dot{\gamma} = 0.04 \text{ sec}^{-1}$.

Based on these results it seems reasonable to conclude that the emulsion particles are destroyed in a bicone geometry under continuous rotation at 190°C, but that the emulsion particles are surprisingly stable. This result is so far in line with the findings of Berens and Volt (20-22). However, the interpretation of the results is not straightforward because slip or melt fracture may occur at the surfaces of the measuring unit.

FLOW CURVES FOR EMULSION POLYMERS

Berens and Volt (20-22) observed what they coined particle flow. Some characteristics for this flow was: flow curves with almost zero slope over large shear rate intervals, very little die swell and emulsion particles discernable in the processed samples.

Fig. 14 show flow curves for an emulsion polymer Vinnol E60 and flow curves for a crosslinked emulsion polymer (a copolymer of divinyl adipate and vinylchloride) compared with the experimental flow curve for a bulk polymer with the same molecular weight distribution as Vinnol E60 and calculated flow curves for monomolecular melts of the two emulsion polymers.

The observed behaviour resembles the phenomena observed when a slip plane is established during powder processing, the melt fracture phenomenon or the boundary lubrication behaviour with constant coefficient of friction. The interpretation of the data is far from obvious. But since it was shown above that the emulsion particles are gradually disintegrated in a constant shear field one might tentatively assume that the main effect involves a breakage of the adhesion to the wall of the measuring unit. This proposal is in line with Pezzins (1) observation that "the limiting shear stress value is rather close to the yield shear stress for particle slippage postulated for PVC resin flow". Anamalous capillary flow of the emulsion polymer Vinnol E60 is also observed in materials where the original particle structure according to electron microscopy is destroyed. This last observation seems to be in accordance with Menning's (46) observation, that particles disappear irreversibly with increasing temperature, whereas "slip" seems to be a reversible phenomenon for the emulsion polymer he studied.

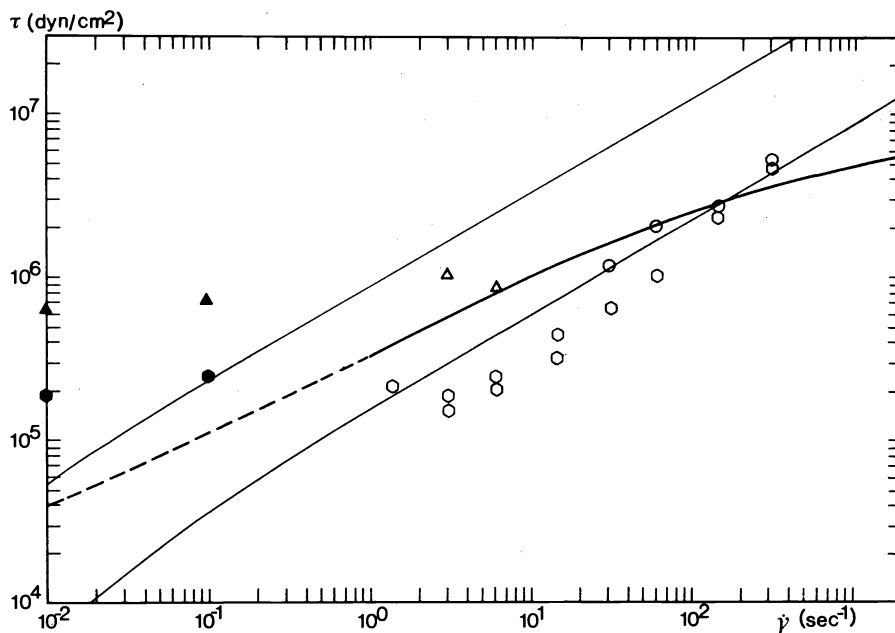


Fig. 14 shows flow curves for an emulsion copolymer of DVA and VCl (polymer E), \blacktriangle measured with the bicone geometry, Δ measured on the Instron Rheometer. \bullet Data measured with the bicone on Vinnol E60 and \circ Instron data. Thin drawn curves are calculated for monomolecular melts with the same molecular weight distributions as Vinnol E60 and polymer E without crosslinks. Heavy full drawn curve has been reported by Wales (45) for a bulk polymer with the same molecular weight distribution as Vinnol E60.

EXPERIMENTAL

Sample Materials

The following materials were used:

- A. A bulk polymerized material Vinnol Y60 a commercial polymer from Wacker, $\bar{M}_w = 74000$, $\bar{M}_n = 35000$.
- B. An emulsion polymer Vinnol E60g from Wacker, same molecular weight distribution as Vinnol Y60.
- C. An emulsion polymer with mean particle size: 0.27μ produced by seed polymerization at 50°C , $\bar{M}_w = 118000$ and $\bar{M}_n = 54000$.
- D. A suspension polymer Vinnol H70d from Wacker with $\bar{M}_w = 110000$ and $\bar{M}_n = 52000$.
- E. A slightly cross-linked copolymer of divinyladipate (DVA) and vinylchloride (VCl) prepared by emulsion polymerization at 40°C to an extent of reaction 81%. The recipe: 480g H_2O , 100g VCl, 1.6g DVA, 0.75g sodium laurate, 0.592g $\text{K}_2\text{S}_2\text{O}_8$. A homopolymer prepared by the same recipe had $\bar{M}_w = 150000$ and $\bar{M}_n = 75000$ determined by GPC.

The average molecular weight of a chain between cross-links was estimated from swell experiments and from the calculated composition of the copolymer to ≈ 7000 . Approx. 50% of the copolymer dissolve in THF before and after processing.

Sintering of the samples were performed in a hydraulic press at $T=120^\circ\text{C}$, $p=100\text{kP/cm}^2$ for two minutes.

The GPC procedure has been described in ref. 26.

Rheometry

The following rheometers were used in this study: An Instron capillary rheometer (Capillary length: 2.0049", Capillary diameter: 0.0289"), a rheometrics mechanical spectrometer, used in both cone and plate mode and in the biconical mode, and finally a Brabender Plastograph (1).

The bicone geometry supplied by Rheometrics (BC-1) was modified with a teflon insert as recommended by Whorlow (47).

When using the bicone geometry the ideal equation relating torque and shear stress has to be corrected for contributions of the cavity walls and shaft hole (47, 48). In this work the relations:

$$\begin{aligned} \tau &= 90 M \\ \gamma &= 10 \omega \end{aligned}$$

where τ is in $\frac{\text{dyn}}{\text{cm}^2}$, M is in g·cm and ω is in radians/sec. were found by calibration.

Electron Microscopy

Scanning electron microscopy was obtained with an instrument from JEOL model JSM-U3. Fracture surfaces were prepared by cooling the samples in liquid nitrogen and then breaking the sample.

The fracture surface is coated with a carbon film and then with palladium or gold; total layer thickness was approximately 300Å.

Transmission electron microscopy was performed with an instrument from JEOL model JEM-100B-TR.

The PMMA embedded samples were prepared by covering a PVC sample with MMA in a small test-tube for 24 hours followed by polymerization at 50°C for 24 hours with AIBN as initiator (1%).

The ultramicrotomic cuts were prepared on an Ultramicrotom OM U3 from Reichert, Austria.

Acknowledgement This work was supported by a grant from Statens Teknisk-Videnskabelige Forskningsråd.

REFERENCES

1. G. Pezzin, Pure Appl. Chem., **26**, 241, (1971).
2. E.A. Collins, Pure Appl. Chem., **49**, 581, (1977).
3. J. Lyngaae-Jørgensen, J. Polym. Sci., C, **33**, 39, (1971).
4. A.H. Abdel-Alim and A.E. Hamielec, J. Appl. Polym. Sci., **16**, 783, (1972).
5. T. Hjertberg and E. Sörvik, J. Polym. Sci., Polym. Chem., **16**, 645, (1978).
6. J. Lyngaae-Jørgensen, Proceedings, 7th Int. Seminar GPC, p 188, (1969).
7. J. Lyngaae-Jørgensen, J. Chromatog. Sci., **9**, 331, (1971).
8. A.J. de Vries, C. Bonnebat and M. Carrega, Pure Appl. Chem., **25**, 209, (1971).
9. R.K.S. Chan and C. Warman, Polym. Eng. Sci., **12**, 209, (1971).
10. K.B. Abbås, F.A. Bovey and F.C. Schilling, Makromol. Chem., Suppl. **1**, 227, (1975).
11. K.B. Abbås, J. Macromol. Sci., Phys., **B14**, 159 (1977).
12. J. Lyngaae-Jørgensen, lic.Tech. (Ph.D.) Thesis, The Technical University of Denmark, (1970).
13. M.E. Carrega, Pure Appl. Chem., **49**, 569, (1977).
14. T. Alfrey, N. Wiederhorn, R. Stein and A. Tobolsky, J. Colloid Sci., **4**, 211, (1949).
15. G. Pezzin, Plastics and Polymers, **37**, 295, (1969).
16. J. Lyngaae-Jørgensen, Macromol. Chem., **167**, 311, (1973).
17. J. Lyngaae-Jørgensen, J. Phys. Chem., **80**, 824, (1976).
18. J.A. Juijn, J.H. Gisolf and W.A. de Jong, Kolloid-Z u. Z. Polymere, **251**, 456, (1973).
19. G. Matthews, Vinyl and Allied Polymers, Vol. 2., Ilife Books, London (1972)
20. A.R. Berens and V.L. Folt, Trans. Soc. Rheol., **11**, 95 (1967).
21. A.R. Berens and V.L. Folt, Polym. Eng. Sci., **8**, 5, (1968).
22. Ibid, **9**, 27, (1969).
23. T. Hattori, K. Tanaka and M. Matsuo, Polym. Eng. Sci., **12**, 199, (1972).
24. J.C. Chauffoureaux, C. Dehennau and J. van Rijckevorsel, J. Rheol., **23**, 1, (1979).
25. R.D. Hoffman and S.Y. Choi, 27' SPE-ANTEC., **15**, 61, (1969).
26. J. Lyngaae-Jørgensen, Polym. Eng. Sci., **14**, 342, (1974).
27. J. Lyngaae-Jørgensen, Relations Between Structure and Rheological Properties of Concentrated Polymer Melts, Thesis, The Technical University of Denmark, (1980).

28. E.A. Collins and C.A. Krier, Trans. Soc. Rheol., 11, 225, (1967).
29. J. Lyngaae-Jørgensen, J. Appl. Polym. Sci., 20, 2497, (1976).
30. L.A. Utracki, J. Polym. Sci., 12, 563, (1974).
31. G.V. Vinogradov, A.Y. Matkin and V.V. Volosevitch, J. Appl. Polym. Sci., Appl. Polym. Symposia, 27, 47, (1975).
32. G.V. Vinogradov, Polymer, 18, 1275, (1977).
33. G.V. Vinogradov, A.I. Isayer, D.A. Mustafaev and Y.Y. Podolsky, J. Appl. Polym. Sci., 22, 665, (1978).
34. G.V. Vinogradov, A.Y. Matkin, V.V. Volosevitch, V.P. Shatalov and V.P. Yudin, J. Polym. Sci., Polym. Phys., 13, 1721, (1975).
35. T.L. Smith, Chapter 4 in: F.R. Eirich, Rheology, Theory and Applications, Vol. 5, Academic Press, (1969).
36. F. Bueche, Physical Properties of Polymers, Interscience, (1962).
37. C. Bonnebat and A.J. de Vries, Polym. Eng. Sci., 18, 824, (1978).
38. N. Nakajima and E.A. Collins, J. Appl. Polym. Sci., 22, 2435, (1978).
39. E. Rasmussen, Laboratory Report from Northern Cable and Wire Works, Copenhagen, private Communication.
40. C.L. Sieglaff., SPE. Transac., 4, 129, (1964).
41. E.A. Collins and A.P. Metzger, Polym. Eng. Sci., 10, 57, (1970).
42. C.L. Sieglaff, Polym. Eng. Sci., 9, 81, (1969).
43. R.N. Hayward and I. Brough, Polymer, 10, 724, (1969).
44. R.N. Hayward, The Physics of Glassy Polymers, Appl. Sci. Publ., (1973).
45. J.L.S. Wales, J. Polym. Sci., Symp. No. 50, 469 (1975).
46. G. Menning, J. Macromol. Sci.-Phys., B14, 231, (1977).
47. P.T. Galvin and R.W. Whorlow, J. Appl. Polym. Sci., (19), 567, (1975).
48. E. Broyer and C.W. Macosko, SPE-ANTEC, 33, 343, (1975).